

Seeing Is Believing: Coupling Between Liquid Crystalline Ordering and Rheological Behaviour in Cellulose Nanocrystals Suspensions

Giuliano Zanchetta^{*a}, Elisa Rocchi^b, Laura Piazza^b

^a Dept. of Medical Biotechnology and Translational Medicine, Università degli Studi di Milano, V. F.lli Cervi 93, Segrate, Italy

^b Dept. of Food, Environmental and Nutritional Sciences, Università degli Studi di Milano, V. Mangiagalli 25, Milano, Italy
giuliano.zanchetta@unimi.it

Nanomaterial engineering technologies have the potential to revolutionize industrial food systems, addressing issues related to health and sustainability. Some nanomaterials have unique physico-chemical properties that can be exploited for beneficial effects on food, leading to increased shelf life, enhanced flavour release, and increased absorption of nutrients and other bioactive components. In food production, processing steps like pipe flow, mixing and evaporation can clearly affect - and be affected by - mesoscopic arrangement of components. A nanomaterial characterization challenge includes the consideration of physico-chemical changes as a nanoscale material moves from formulation through incorporation into final products. These complexities could include the effective nanomaterial size, physical state, and behaviour under stress, which is quantified in terms of rheological performance.

Here, we investigate the interplay between ordering and rheological behaviour in suspensions of Cellulose Nanocrystals (CNC) extracted with acid hydrolysis from plant biomass waste. In particular, through a microscopy shear cell we gain access to CNC textures and local degree of alignment upon oscillatory deformations, and compare them with linear and nonlinear rheological response.

We find that, within the liquid crystalline and gel phases of CNC, some of the pre-shear protocols typically used in rheological measurements - involving mechanical yielding imposed via large amplitude oscillations or continuous shear - are associated to perturbation and persistent alignment of CNC domains along the shear direction, which in turn weaken the linear mechanical CNC response. Complete relaxation of shear-induced ordering and full recovery of linear moduli only occur over hundreds of seconds. We thus show that the combination of optical and rheological characterization can provide a valuable tool for the assessment of non-linear behaviour in complex fluids like CNC suspensions.

1. Introduction

Cellulose is the most abundant biopolymer on Earth, and has traditionally been extracted from plant cell walls in the form of fibres and microfibrils (Portela et al., 2015) mainly for paper and clothing manufacturing.

More recently, methods based on hydrolysis have been developed, which allow to separate crystalline regions from amorphous ones (Bondeson et al., 2006). Cellulose Nano Crystals (CNC) are chiral, elongated particles whose size and surface charge can be tuned through a proper choice of the protocol; they feature excellent mechanical and optical properties and versatile surface chemistry. Such interesting features, together with the possibility of extracting CNC from a variety of sustainable sources (Gonçalves et al., 2016), open new routes for applications ranging from light materials to reinforcing additives to photonics; in particular, in the food technology, CNCs are explored for use in packaging and in formulation, as texturizing agents or carriers of aromatic substances. CNC as a natural emulsifying and stabilizing ingredient is of great interest in food products such as salad dressings, whipped toppings, sauces, foams, soups, puddings, dips (Gómez et al., 2016). As an example, emulsions can be formed and stabilized not only by surface-active compounds, such as surfactants or proteins, but also by solid particles to form "Pickering emulsions". Bio-based particles like

CNC are suitable options to develop Pickering emulsions. They allow for the manufacture of environmentally friendly materials and can provide a wide range of aspect ratios and lengths (Cunha et al., 2014).

Many of such applications critically depend on the control of phase behaviour of CNC dilute and concentrated aqueous dispersions, on their mechanical properties and on the effects of processing steps. Indeed, due to their anisotropic shape, repulsive interactions and intrinsic chirality, CNCs feature a transition from an isotropic solution to a partially ordered fluid state, called chiral nematic or cholesteric (N^*) liquid crystalline phase. N^* phase is characterized by orientational order and optical anisotropy, or birefringence, and by an additional periodicity at the micrometre scale due to the chirality of the single CNCs. The critical concentration c_{CNC} for such a transition primarily depends on CNC aspect ratio and surface charge. At further higher c_{CNC} , solutions - while retaining their partial ordering - get kinetically arrested and enter a metastable phase commonly called gel for its rheological properties (Klemm et al., 2011; Lagerwall et al., 2014). However, since the main driving force for the kinetic arrest is the electrostatic repulsive interaction between CNCs, such phase is more properly defined as glassy.

Clearly, the degree of ordering of the CNCs can impact their mechanical response; viceversa, some non-linear rheological tests, like large amplitude oscillations or continuous shear – together with typical processing steps like pipe flow or drying – can profoundly affect their ordering degree. This raises the need of a proper assessment of pre-shearing protocols for reliable measurements. Therefore, we address here the interplay among large deformations, degree of ordering, and measurements of the mechanical properties of partially oriented samples, by comparing rheological tests and the appearance and degree of ordering of CNC textures, via a microscope-based shear cell coupled to a fast camera. To this aim, we mainly focus on a CNC sample at high c_{CNC} , exploring the range across the transition between N^* and gel phase.

2. Materials and methods

2.1 Materials and sample preparation

CNCs samples, a kind gift of D. Kam (Hebrew University of Jerusalem), were obtained from waste cellulosic material (from paper industry), following an established protocol which involves sulfuric acid hydrolysis, washing and sonication steps (Bondeson et al., 2006; Abraham et al., 2016).

The CNC sample described here has been characterized via Dynamic Light Scattering, Atomic Force Microscopy and cryogenic Transmission Electron Microscopy to determine CNC size; relatively narrow distributions have been found, with average length $L = 100$ nm (90 % between 50 and 175 nm) and average diameter $D = 5.5$ nm (90 % between 3 and 8 nm). The presence of aggregates was detected, possibly due to low sonication time/power. Surface charge, as determined by Zeta Potential, is -0.237 e/nm². The stock solution, 5.9 % in weight, was diluted with milliQ water to obtain lower c_{CNC} samples.

2.2 Rheological and rheo-optical characterization

Rheological measurements, oscillatory and continuous shear, were performed with a DHR-2 rheometer (TA Instruments) equipped with 40 mm diameter cone-plate geometry, with a gap of 28 μ m. Care was taken that samples were fully homogenous within the timescale of measurements.

Rheo-optical characterization was performed on a RheoOptiCAD cell (CAD Instruments), a linear, strain-controlled shearing device coupled to a Nikon Ti-S inverted microscope and a CCD camera (AVT Prosilica GX1050), which allows both transmission and reflection imaging. A low, 2x magnification was chosen to ensure a large field of view; two crossed polarizers were inserted along the optical path, before and after the sample, at 45 degrees relative to shearing direction to maximize sensitivity to optical anisotropy. Two glass slides confined the sample within a gap of 200 μ m. Stacks of images were acquired at 20-50 fps via Labview custom software and processed via ImageJ or custom Matlab code. Both types of measurements were performed at 25 °C.

3. Results and discussion

3.1 Phase diagram

We evaluated the phase diagram via a combination of macroscopic and polarized optical microscopy observations, finding the expected transition from isotropic to coexisting isotropic and N^* phases at $c_{CNC} = 2.5$ %. In Figure 1 we report the fraction of N^* phase Φ_{N^*} as a function of c_{CNC} , together with microscope textures showing the characteristic stripes of N^* phase in coexistence with isotropic. For $c_{CNC} > 5$ %, when Φ_{N^*} is still lower than unity, the macroscopic interface gets fuzzy and phase separation is completely suppressed at $c_{CNC} = 5.9$ %. Correspondingly, microscopy textures get “frozen” and show increased birefringence, along with

disappearance of detectable N^* periodicity. Such observations mark the appearance of a kinetically arrested phase, in which N^* regions are supposedly jammed.

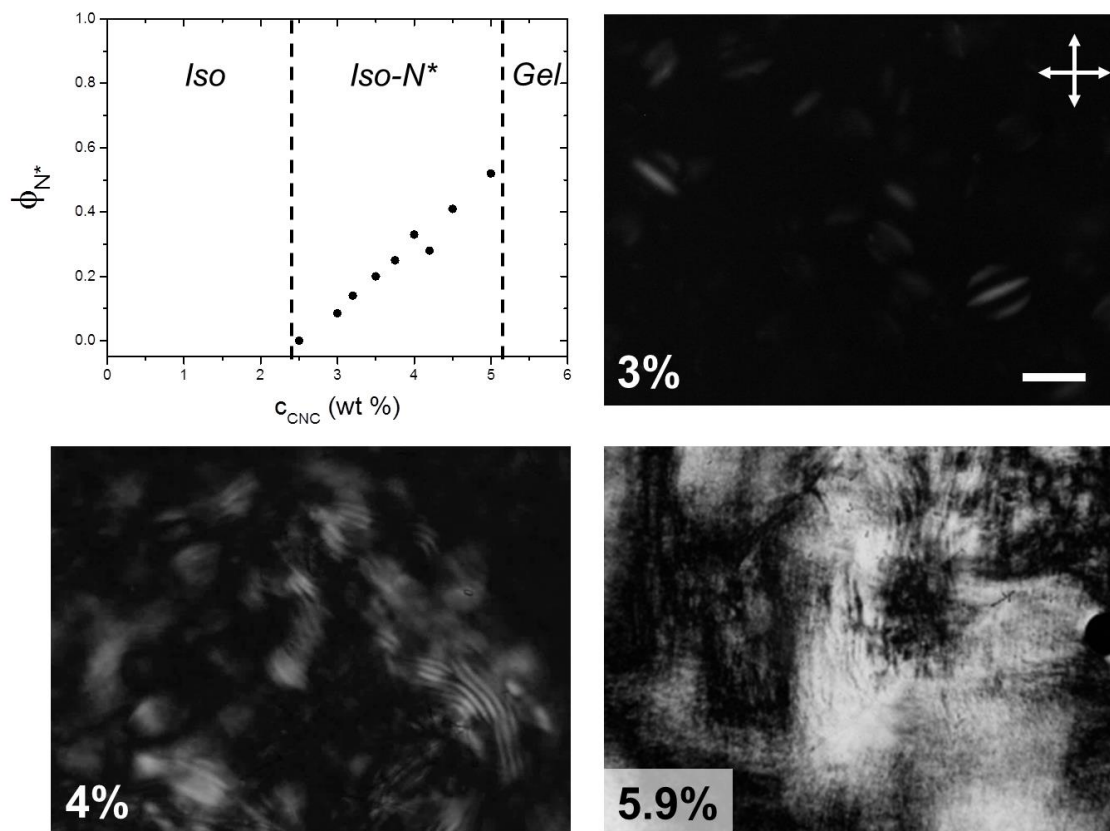


Figure 1: CNC phase diagram. Top left: volume fraction of N^* phase as a function of CNC concentration. Other panels show typical polarized microscopy textures for the indicated concentrations. Size bar: 20 μm .

3.2 Linear and non-linear rheological characterization

Materials that contain more than one phase can be considered structured fluids since their rheological behaviour is affected by the interactions of the constituents. We performed linear oscillatory rheology measurements in the same c_{CNC} range. In Figure 2a, we show the storage modulus G' and loss modulus G'' as a function of frequency. For samples up to 5 %, the mechanical response is mostly fluid-like, with a non-negligible elastic component, yet vanishing at low frequency. On the contrary, for $c_{\text{CNC}} = 5.9$ %, CNC behaviour shows a clear discontinuity, consistent with macroscopic and microscopic observations: G' prevails over G'' and becomes nearly frequency-independent. Some of these features are reminiscent of critical gels (characterized by similar power-law scaling of G' and G'' with frequency), which consist of minimally connected structures; however, at this stage it is not yet clear if the presence of aggregates play any role in such behaviour.

We also explored the effect of large deformations, as shown in Figure 2b. Upon increasing c_{CNC} , both the limit of linear response region and the yielding strain (where G' equals G'') increase, up to 10% and 200-300 %, respectively.

3.3 Coupling between rheological response and degree of ordering

Within the Iso- N^* region, different pre-shearing protocols yield similar and reproducible effects (data not shown). On the contrary, at $c_{\text{CNC}} = 5.9$ %, i.e. within the kinetically arrested phase, we observed a marked dependence of the measured linear moduli on the type and extent of pre-shear. In Figure 3a, we show linear frequency sweep measurements for the same sample, either only allowed to relax for 15 minutes after loading, or subjected to different deformations and immediately tested after pre-treatment. While 100% oscillations produce only slight weakening of the elastic response, 300% oscillations and continuous shear at high shear rate dramatically impact sample properties, which only recover after several tens of minutes.

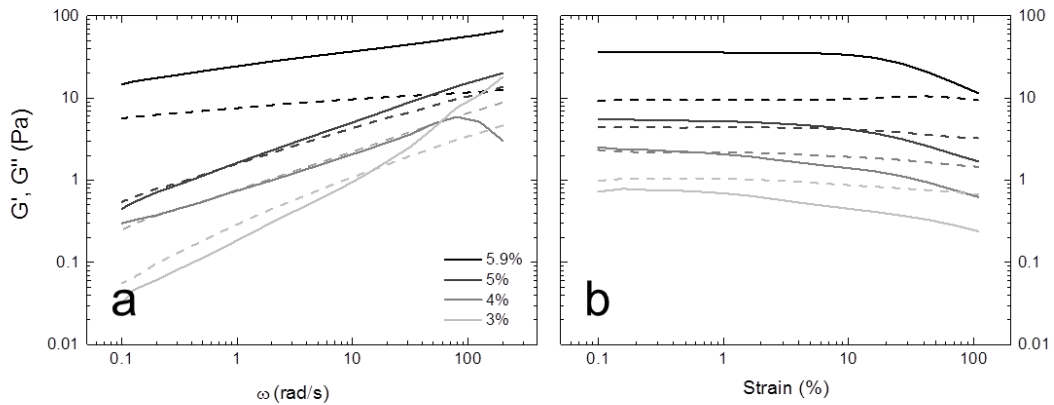


Figure 2: Linear and non-linear rheology. Storage modulus G' (continuous lines) and loss modulus G'' (dashed lines) as a function of angular frequency (panel a, 0.5% amplitude) and oscillation amplitude (b, 10 rad/s), for various CNC concentrations.

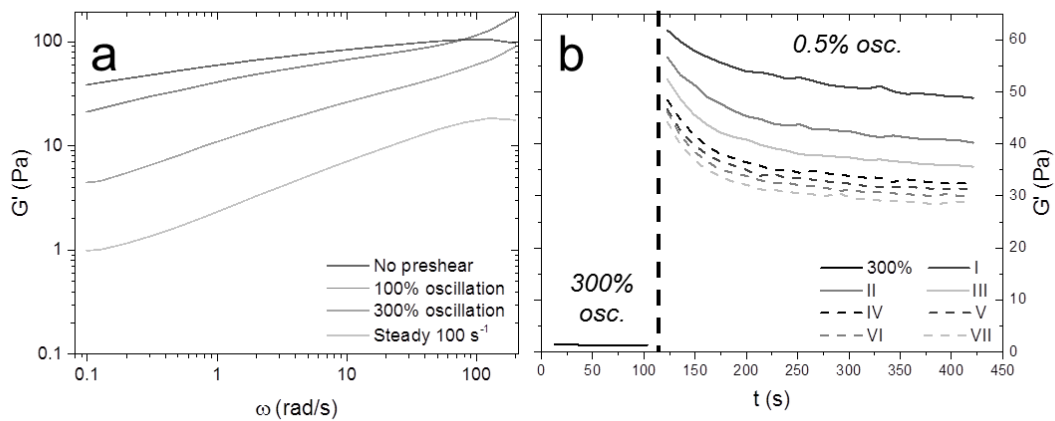


Figure 3: History dependence. (a) Frequency dependence of G' for different pre-shearing protocols. (b) Measured G' for a 300% oscillation and linear response during recovery time, for various consecutive cycles.

Furthermore, Figure 3b displays the measured G' during a non-linear, 300 % oscillation and its time evolution (as measured through a linear 0.5 % oscillation) during the subsequent 300 seconds interval, for several repeated cycles. An almost immediate G' recovery is observed after each cessation, followed by a slow relaxation to a plateau value. Overall, the effect of each cycle of large oscillations adds to the previous one with a progressive weakening effect.

To better understand the correlation between shear history and measured mechanical properties, we should consider the microstructure of the system. The arrested phase of CNC is made up by a large fraction of partially ordered, tightly packed N^* domains (which however cannot be singularly resolved). Therefore, a possible contribution to the elasticity of the phase may come from networks of defects between neighbouring domains. Indeed, a significant interplay between defects and shear properties has been reported for LC polymers like PBLG and Hydroxypropyl Cellulose (Echeverria et al., 2015) and in thermotropic LCs (Ramos et al., 2002).

To get better insight into CNC arrangement and response, we placed the high c_{CNC} sample in a microscope shear cell and observed it during different applied deformations. Polarized microscopy allows to highlight the extent and spatial distribution of birefringent, i.e. aligned, regions. We chose a low magnification to access a large portion of the sample, at the expenses of spatial resolution. Furthermore, since the response of the sample is rather uniform across the field of view, to estimate the effect of deformations on the overall degree

of alignment we extracted from each image the average intensity I_T of light transmitted through the crossed polarizers. I_T would be expected to be nearly zero for a quiescent isotropic sample (or for a set of perfectly disordered domains). This is clearly not the case for our sample, which shows a significant birefringence in the gel phase (see Figure 1), possibly resulting from domains sheared and aligned upon cell loading, and from structuring at substrates. In any case, the relative variation of I_T can provide a meaningful estimate of sample alignment evolution.

We subjected CNC to oscillatory deformations at various amplitudes, ranging from linear to strongly non-linear regimes. Because the system is not a simple dispersion of independent rods but rather it is composed by jammed N^* domains, the optical response to deformation is a complex phenomenon, resulting from the combination of mechanical resistance and yielding, tendency to align along the shear direction, and ongoing relaxation phenomena. This non-trivial behaviour can be appreciated in the inset of Figure 4, which shows the transmitted intensity at start-up for a 300% oscillation. However, we are here interested in the resulting effect of deformations on the time scale of seconds to minutes relevant for rheology experiments and for typical processing steps like pipe flow or blade mixing; therefore, we average I_T over the oscillation period.

In Figure 4, we report the time evolution of the averaged I_T during and after the applied deformation for different amplitudes. Oscillations with amplitudes in the linear regime and amplitudes slightly below yield strain *reduce* the overall intensity, which we can attribute to partial relaxation of previous, “frozen” alignment. Instead, for amplitudes at yield strain and above, during the application of oscillations I_T grows and reaches a plateau within few seconds, corresponding to fluidization of the sample and further alignment of N^* regions, which partially relaxes after stopping the oscillation. Small oscillations bring the sample to a lower degree of order and only slightly affect the defect network; large oscillations increase the overall alignment and push the sample towards a well-aligned, thermodynamically stable N^* phase, which however has weaker elastic component.

When looking for an appropriate pre-shear protocol for complex anisotropic samples like CNC at high concentration, one should thus consider what kind of material and what kind of phase - stable or metastable, isotropic or anisotropic - has to be measured. Reproducibility of linear tests may not be enough to ensure that the system is not affected by the shear itself. For the gel phase of CNC, our measurements suggest that oscillations with amplitude around the yield strain may provide the best compromise between fluidization and imposed alignment.

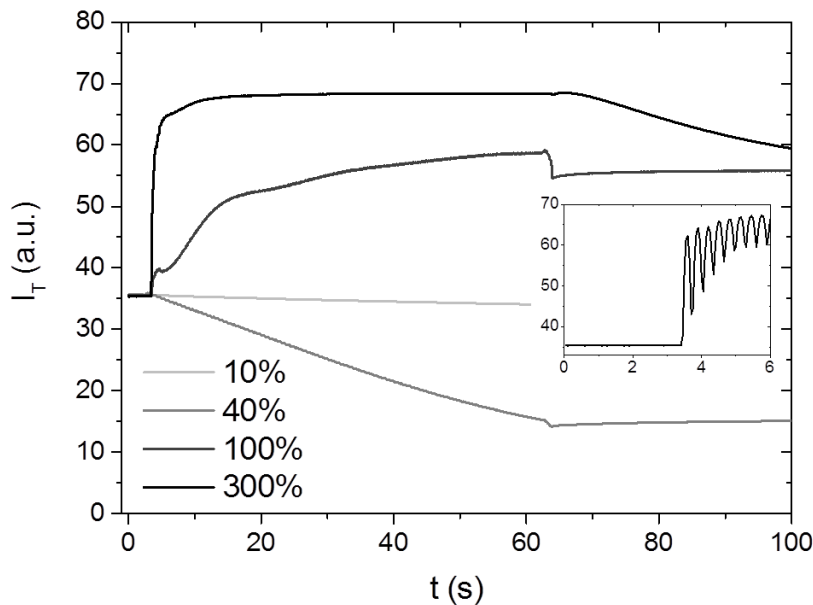


Figure 4: Transmitted intensity I_T through crossed polarizers for CNC at 5.9 %, during oscillations at different amplitudes and after cessation. I_T is averaged over each oscillation period. Inset: non-averaged I_T for the start-up at 300 %.

4. Conclusions

We combined rheological measurements and microscopy observations under shear to characterize the N* and gel phases of CNC dispersion. In particular, we investigated the correlation between the degree of alignment and the elasticity of the phase. We found that large and fast deformations, typically applied in colloidal gels to rejuvenate the samples, in CNC anisotropic phases promote sample alignment which in turn lowers its mechanical properties. In such situations, optical access to the sheared textures can prove extremely beneficial to establish reliable protocols.

Acknowledgments

We acknowledge the kind gift of CNC samples from D. Kam (Hebrew University of Jerusalem).

Reference

- Abraham E., Kam D., Nevo Y., Slattegard R., Rivkin A., Lapidot S., Shoseyov O., 2016, Highly Modified Cellulose Nanocrystals and Formation of EpoxyNanocrystalline Cellulose (CNC) Nanocomposites, *ACS Appl. Mater. Interfaces*, 8, 28086-28095.
- Bondeson D., Mathew A., Oksman K., 2006, Optimization of the Isolation of Nanocrystals from Microcrystalline Cellulose by Acid Hydrolysis, *Cellulose*, 13, 171-180.
- Cunha A. G., Mougél J.-B., Cathala B., Berglund L., Capron I., 2014, Preparation of double Pickering emulsions stabilized by chemically tailored nanocelluloses, *Langmuir*, 30, 9327-9335.
- Echeverria C., Almeida P. L., Feioa G., Figueirinhas J. L., Rey A. D., Godinho M. H., 2015, Rheo-NMR study of water-based cellulose liquid crystal system at high shear rates, *Polymer*, 65, 18-25.
- Gómez C. H., Serpa A., Velásquez-Cock J., Gañán P., Castro C., Vélez L., Zuluaga R., 2016, Vegetable nanocellulose in food science: A review, *Food Hydrocolloids*, 57, 178-186.
- Gonçalves A. P. B., Cruz A. M. F., de Sales J. C., Souza M. C., da Silva F. L. B. M, Guimarães F. L. B. M, Mattedia S., José N. M., 2016, Achievement and Characterization of Cellulose Nanowhiskers of Palm (*Elaeis Guineensis*) and Bromelia Fibers (*Neoglaziovia Variegata*), *Chemical Engineering Transactions*, 50, 403-408.
- Klemm D., Kramer F., Moritz S., Lindström T., Ankerfors M., Gray D., Dorris A., 2011, Nanocelluloses: A New Family of Nature-Based Materials, *Angew. Chem. Int. Ed.*, 50, 5438-5466.
- Lagerwall J. P. F., Schütz C., Salajkova M., Noh J., Park J. H., Scalia G., Bergström L., 2014, Cellulose nanocrystal-based materials: from liquid crystal self-assembly and glass formation to multifunctional thin films, *NPG Asia Materials*, 6, e80.
- Portela I., González Alriols M., Labidi J., Llano-Ponte R., 2015, Cellulose Nanofibers from Recycled Cellulose Pulp, *Chemical Engineering Transactions*, 45, 937-942.
- Ramos L., Zapotocky M., Lubensky T. C., Weitz D. A., 2002, Rheology of defect networks in cholesteric liquid crystals, *Phys. Rev. E*, 66, 031711.